ShockWaves manuscript No.
(will be inserted by the editor)

High-speed time-resolved color schlieren visualization of shock wave phenomena

H. Kleine[1], K. Hiraki[2], H. Maruyama[3], T. Hayashida[3], J. Yonai[3], K. Kitamura[3], Y. Kondo[4], and T.G. Etoh[5]

[1] School of Aerospace, Civil and Mechanical Engineering, University College, University of New South Wales/Australian Defence Force Academy, Canberra, ACT 2600, Australia
[2] Department of Mechanical and Control Engineering, Faculty of Engineering, Kyushu Institute of Technology, Kita-Kyushu, 804-8550 Japan
[3] Science & Technical Research Laboratories, NHK (Japan Broadcasting Corporation), Tokyo, 157-8510 Japan
[4] Research & Development Group, Analytical and Measuring Instruments Division, Shimadzu Corporation, Kyoto, 604-8511 Japan
[5] Department of Civil Engineering, Graduate School of Science and Engineering, Kinki University, Osaka, 577-8502 Japan

Received: date / Revised version: date

Abstract. A newly developed high-speed color video camera, which can record 103 frames at rates of up to one million frames per second, has been used to obtain time-resolved color schlieren visualizations of shock wave phenomena. These trials constitute the first successful time-resolved application of the direction-indicating color schlieren method with frame rates up to 125 kHz. The instabilities of a supersonic flow over a double cone were made visible in unprecedented clarity, and the potential of the camera for schlieren visualizations was further demonstrated in experiments showing the explosion of a small firecracker and the bursting of a helium-filled toy balloon.

Key words: High-speed video camera, Density-sensitive flow visualization techniques, Flow instabilities, Blast waves

1 Introduction

The methods of high-speed photography are used when the phenomenon to be observed or visualized occurs too quickly for normal human perception. Historically, this discipline was created in parallel to the development of general photography. The first high-speed photography records were already obtained in the middle of the 19th century, about ten years after successful photographic procedures were established (Fuller 1997).

The first approach to the problem was to take a single picture of a transient event, 'freezing' a single instant of the motion. For relatively slow moving objects, a mechanical shutter can suffice to provide an adequately small exposure time to stop the motion. Faster events, however, are usually imaged with an open shutter camera, where an adequately timed flash exposes the film, the exposure time being equal to the duration of the flash. This technique was, in fact, developed before proper mechanical shutters became available, and first results were published as early as 1852 (Fuller 1997).

Figure 1 presents an example of such a single-shot open-shutter high-speed photograph. If the observed process is highly reproducible, a complete sequence of the event can be obtained by repeating it several times and taking the image at different instants, that is, by continuously increasing the delay between the start of the process and the moment of photography. This technique, which is still used in many laboratories all over the world, can yield

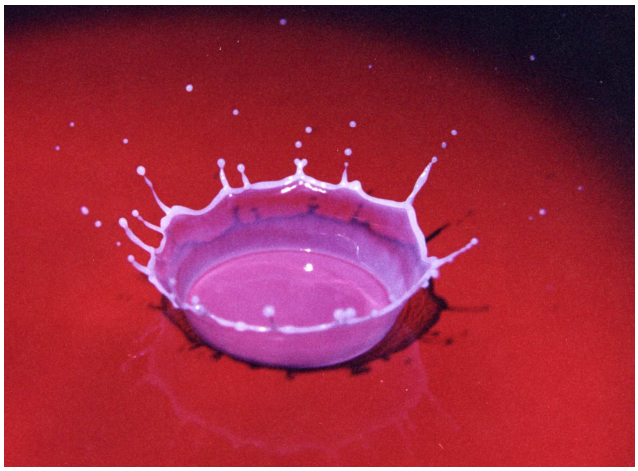

Fig. 1. Open-shutter photograph of a milk drop hitting a smooth surface covered with a thin layer of milk; exposure by spark light source, exposure time approx. 2 μs

Correspondence to: H. Kleine (e-mail: h.kleine@adfa.edu.au)

high-resolution images of the event, with different visualization methods, and on a wide range of recording materials. Since this approach only yields one image per event, its usefulness is restricted to processes that exhibit the aforementioned high degree of repeatability. Any process that is not fully repeatable, e.g., a process that includes random elements such as instabilities, cannot be adequately represented by images obtained with the described single-shot method, even if the initial conditions of the event are exactly reproduced. The splashing of a milk drop seen in Fig. 1 belongs to this category, even though some main features of the process such as size and formation time of the 'crown' are largely reproducible. Smaller structures such as the observed break-up pattern of tiny droplets at the rim of the splashed liquid, however, are impossible to repeat exactly, even if the mass of the drop and its impact velocity are precisely controlled and reproduced.

For processes of this type, high-speed photography with multiple still images or high-speed cine photography is required. These techniques were developed shortly after first demonstrations of the single-shot method. An often-quoted example is the work of English/American engineer Eadweard Muybridge, who, among other pioneering observations of high-speed motion, verified in 1872, by using multiple cameras, that a trotting horse had all four feet off the ground at some instants during its movement (Fuller 1997). Towards the end of the 19th century, cine cameras were developed, and the first successful high-speed cine films were obtained in the 1930s. Since then, a large number of systems has been devised and built, some of which were designed for very specific purposes and applications. In addition to the numerous custom-made systems created by various laboratories interested in high-speed events, a range of commercial cameras for high-speed photography has become available since the middle of the last century. Overviews of techniques and equipment are given, for example, in the book edited by Ray (1997).

Over the last three decades, electronically accessible media in the form of magnetic tapes and eventually charge-coupled device (CCD) chips have started to compete with photographic film as the recording material (Balch 1997). The arguably predominant benefit of having the images immediately available and accessible in electronic form is partially offset by a loss in resolution, as the number of pixels on a CCD chip is still no match for the myriad of silver halogen molecule compounds of photographic film. This obvious drawback has, however, been largely compensated by the advances in modern computer chip technology, which have not only led to a significant reduction in size and bulk of the camera systems, but also to significantly improved user-friendly operation characteristics. An electronic recording medium has therefore become a standard feature of almost all new high-speed cameras developed over the last decade. Image converter cameras (Honour 2000) and high-speed digital video systems (Balch 1997, Etoh et al. 2000) represent two current commercially available groups of cameras, which find increasingly frequent application and which slowly replace most film-based high-speed cine apparatuses.

Even though detailed discussions of the observed transient processes will most likely be based on a frame-by-frame analysis, an animated display – essentially an extreme slow motion movie – has invaluable benefits for a qualitative phenomenological description of the process. This was already recognized in the early development of high-speed photography, and such motion picture sequences were created by several laboratories from records obtained with multiple-image devices such as rotating mirror cameras or Cranz-Schardin systems (e.g., Reichenbach 1981). In more recent times, animated displays from sequences of single-shot results of highly repeatable processes were also introduced (Abe et al. 1999). The creation of these clips usually involved a large amount of – often manual – post-processing to match the frames with respect to field of view and exposure level. For systems with a single fixed electronic recording element, such as video cameras, this process is greatly facilitated and is almost exclusively performed in fully automated mode by the system's computer. The high-speed video camera is thus well suited to provide highly informative movie sequences that can help to give the observer a good first understanding of the investigated phenomenon.

In spite of the obvious significance that time-resolved high-speed photography has for the investigation of transient events and in spite of the numerous developments of camera systems, research involving high-speed cine observations/visualizations is still relatively sparse. This is due to mainly four reasons: commercial cameras are considerably expensive and in addition, all time-resolved camera systems generally increase the level of complexity of the experimental/optical apparatus needed for the investigation. Compared to the components that one would use for single-shot observation, a camera for time-resolved recording is often bulky and may be difficult to align. In particular, most film-based cameras may require specially trained personnel with considerable experience in optical systems for an efficient and successful operation. This aspect has become less critical with the advent of smaller, more compact and more user-friendly electronic cameras. Two additional, and potentially more crucial items to consider are that the results of a time-resolved observation/visualization are always inferior in quality compared to single-shot images, and that some valuable visualization techniques, such as holographic interferometry, cannot be readily used in time-resolved mode.

In time-resolved recording, the gain in temporal information is often offset by occasionally substantial losses in spatial resolution, as illustrated in Fig. 2. In this example, the electronically recorded image has a significantly lower resolution than an identically taken single-shot photograph, in spite of the fact that the effective exposure time of the electronic recording amounted only to 30 % of the duration of the flash that exposed the film. The latter fact proves that motion blur is usually not the reason for the limited spatial resolution. This example indicates that on one hand important new information may be gained by time-resolved imaging (i.e., one obtains the time history of an event), but that on the other hand information about

smaller structures and details within the process may be lost.

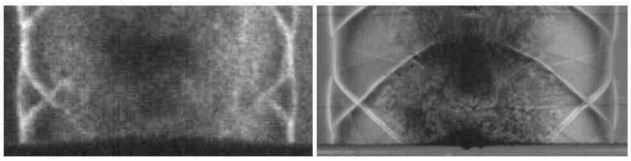

Fig. 2. Detail of the flow field established after the simultaneous explosion of two small explosive charges, visualized by an omnidirectional schlieren method. Left: recorded with an image converter camera, exposure time 300 ns. Right: recorded on 400 ASA film with the open-shutter technique, exposure time 1 μs [from Kleine and Takayama 2001].

In the electronic cine photography systems that have been used prior to the most recent developments described later on, two factors are responsible for losses in spatial resolution. In addition to the relatively small number of pixels of the recording CCD chip, another limiting factor is introduced when high framing rates are to be achieved. A normal, once exposed CCD chip is only available for the next exposure (or frame) after the image signal of the first exposure has been removed and stored in the electronic memory. This transfer time is of the order of several tens to hundreds of microseconds, depending on the size of the exposed pixel array. High framing rates can therefore only be achieved by changing to a partial frame mode, i.e., only a portion of the light-sensitive sensor is exposed. This simply reduces the amount of information to be transferred and thus the transfer time. Consequently, higher frame acquisition rates can be achieved, but the maximum frame rate up to which imaging with a reasonable magnification and resolution is still possible, usually lies well below 100 000 fps (frames per second). The fifth-generation motion analyzer KODAK Ekta-Pro HS4540, one of the fastest video systems developed in the 1990s (Etoh 1992, Balch 1997), can only use 12.5 % of the available chip area when operated at its maximum frame rate of 40 500 fps (see Fig. 3). If only a portion of the CCD chip is available for exposure, the observed object has to be imaged with a smaller magnification factor. This, in conjunction with the limited number of pixels on the receiving CCD chip, further reduces the spatial resolution of the image and makes it difficult, if not impossible, to observe details of the investigated object or process. The switch to partial frame mode for framing rates larger than about 4000 fps has arguably been the most significant disadvantage of previous conventional high-speed video systems.

During the last decade, new technologies have been developed that have improved the performance of CCD chips, in particular with respect to the transfer time required to make the chip available for a subsequent exposure. This work has now culminated in the development of two novel high-speed digital cameras, which can record a sequence with a total of 103 images at framing rates of up to 10^6 fps in full-frame mode (Etoh et al. 2000, 2002). Initially, a monochrome version of this new camera type was developed and tested. The performance of this camera was found to be clearly superior to all other electronic and also film-based high-speed cine cameras, as is illustrated in Fig. 4, which shows the same flow field as Fig. 3, but recorded with the new camera. Even though the chip features the relatively modest number of 81 120 pixels (commercially available single image digital cameras have pixel arrays that are two orders of magnitude larger), the images obtained with this camera are marked by high resolution and outstanding quality.

Following the development of the monochrome version, a color camera using the same type of CCD elements was devised and built (Maruyama et al. 2004). It is the purpose of the present paper to show that this new high-speed color camera can deliver outstanding results when used for the investigation of shock wave phenomena by means of color schlieren visualization. To the best of the authors' knowledge, no time-resolved applications of the direction-indicating color schlieren technique with frame rates exceeding 1000 fps have been achieved prior to these tests.

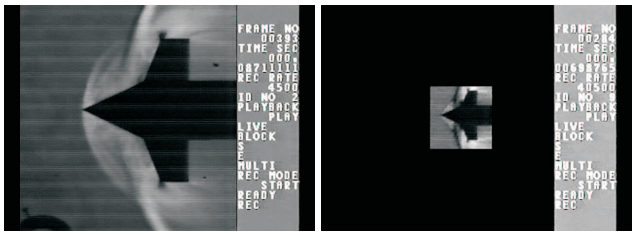

Fig. 3. Visualization of the flow over a double cone model by means of a monochrome omnidirectional schlieren method. Recorded with the fifth-generation motion analyzer KODAK Ekta-Pro HS4540, one of the fastest high-speed video systems developed in the 1990s. Left: Full-frame recording at 4500 fps. Due to an exposure time of several hundreds of microseconds, only a blurred image of the flow field can be obtained. Right: Partial-frame recording at 40 500 fps. The exposure time is short enough to 'freeze' the transient flow, but due to the substantial reduction in size, no details of the flow structure are discernible.

2 Camera performance

The heart of the new high-speed video cameras is an In-Situ Storage Image Sensor (ISIS) CCD chip (Etoh et al. 2000, 2002). This chip features 312 × 260 pixels, each with a 10 bit range, which leads to a file size of 80.12 kByte/frame. Each pixel has its own storage area located within or adjacent to the pixel, with a memory that is sufficiently large to store enough image signals for the generation of a moving image. The transfer time of the image signal to the in-situ storage is considerably less than one microsecond. During the image capturing phase, the image signals are transferred to the in-situ storage but not read out to outside memory. Thus the achievable frame rate is solely governed by the internal transfer time between each

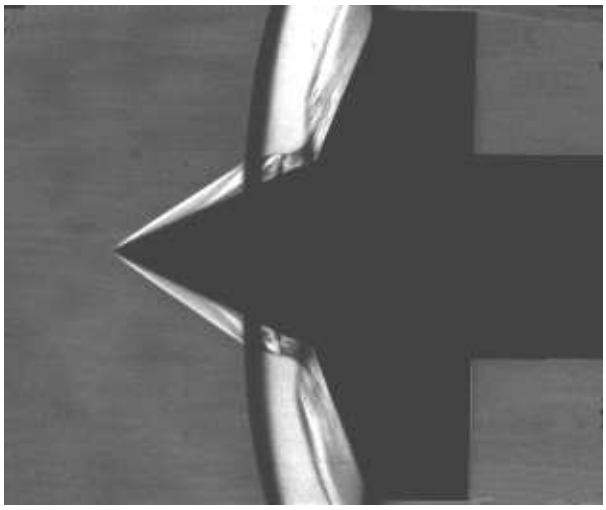

Fig. 4. Visualization of the same flow over the same double cone model as shown in Fig. 3, but with the new Shimadzu high-speed video camera at 62 500 fps.

pixel and its in-situ storage, and is therefore independent of the overall pixel number and thus frame size, unlike the previous systems described in section 1. Further details on the different versions of ISIS CCDs developed so far are given in Etoh et al. (2000). The latest sensor that has further improved performance data and that will be implemented in future high-speed video cameras is described in Etoh et al. (2004). The design of the presently available chip allows one to take and store 103 frames with framing rates up to 10^6 fps; in all cases the full frame is used. The exposure time can be chosen as a fraction ($\frac{1}{2}, \frac{1}{4}$, or $\frac{1}{8}$) of the frame interval. The gain factor can have values between unity and thirty. In the monochrome version of the camera, which is produced by Shimadzu Corp. and which will be commercially available in 2005/2006, recorded sequences can be displayed as AVI files with speeds between 1 fps and 30 fps. Individual images of the sequence can be stored as TIF, JPEG or BMP files. Basic image processing functions (brightness/contrast manipulation) are included in the operating program of the camera.

Image acquisition (and thus triggering) of the camera follows the same working principle as data acquisition with a digital oscilloscope: once armed, the system continuously records and overwrites the in-situ image storage, until an adequate trigger signal initiates the final recording cycle and the subsequent transfer to external memory. It is therefore possible to run the camera in pre-trigger mode, i.e., the recording starts before the actual event of interest has occurred. If the camera has to be synchronized with a pulsed light source, an operation in pre-trigger mode usually requires a separate and independent trigger signal for the light source to accommodate the finite rise time to obtain sufficient light output. If events are observed in which such an independent second trigger signal cannot be provided (as in the example of the balloon burst described later on), and if the observation cannot be made with continuous illumination, operation in the pre-trigger mode is not possible and the recording can only be triggered by the event itself. Other features of the camera, which were, however, of lesser importance for the described applications, include the ability to change frame rates during one recording cycle.

This camera system is unique and easily outperforms all similar high-speed photography equipment, as recent applications (e.g., Dewey and Kleine 2004) have shown. In a brief study conducted in 2002, a prototype of the new monochrome video camera was used and evaluated under typical test conditions for the visualization of unsteady shock waves in air and water. It was possible to perform a direct comparison between the high-speed video camera and a state-of-the-art image converter camera (IMACON 200 by DRS Hadland) – the same phenomenon was observed, using the same optical system, but different cameras (Kleine and Takayama 2002). Both cameras were used to visualize the flow field established by the explosion of a charge above a partially perforated plate (Fig. 5). A typical Mach reflection pattern is formed, while on the left hand side of the charge a portion of the blast wave propagates through the holes in the plate and establishes a series of weaker hemispherical waves each followed by a vortex ring. All flow features are clearly visible on the high-speed video record despite the occasionally obvious effect of the limited number of pixels. Even small-scale structures such as the traces of charge fragments penetrating the leading blast wave can be discerned. In contrast to this, the image converter camera record can only display the major flow elements in an overall fuzzier image, in spite of being recorded on a CCD with a sixteen times higher spatial resolution (1280×1024 pixels).

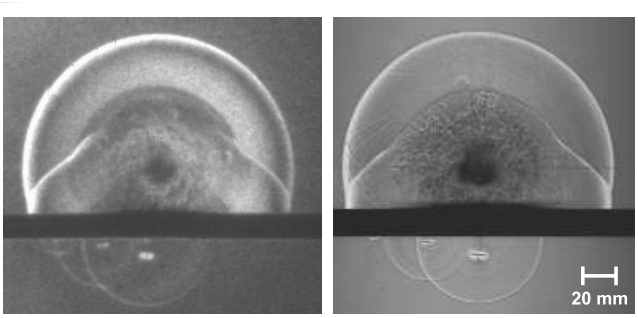

Fig. 5. Direct comparison of the performance of an image converter camera (left; DRS Hadland, IMACON 200) and the Shimadzu high-speed digital camera (right). The visualized flow field shows a blast wave generated 25 mm above a solid plate that has three discrete perforations of 5 mm in diameter on the left hand side (from Kleine and Takayama 2002).

To put the performance data into proper perspective, it should be mentioned that competing systems like CMOS APS sensors can provide higher resolution, but can only be operated in full-frame mode at significantly lower framing rates (typically 500 fps). The aforementioned image converter cameras can achieve framing rates up to $2 \cdot 10^7$ fps, but can only operate in monochrome mode and provide substantially fewer frames (typically 8 to 16) with clearly inferior image resolution, as shown in Figs. 2 and 5.

The color camera consists of three recording units, each of which is equipped with an ISIS CCD identical to the one in the monochrome camera (Maruyama et al. 2004). The incoming light is separated according to color into three signals (R, G, B) by means of a beam splitter prism and each unit records the corresponding signal in one specific color. After recording, the three signals are recombined to form a color image. The settings for frame rate, gain and exposure time are handled equivalently to the monochrome camera version, while the synchronization of all three signal channels is controlled by the system's computer. Because of the separation into the fundamental colors, the camera requires about four times as much light as the monochrome version in order to compensate for the losses at the beam splitter. This poses, however, no serious problem, if an adequately strong light source is used. For the trials described here, the light output of a powerful flashgun for regular photography (Metz Mecablitz 45CT-5) was sufficient.

Further improvement of the camera can be expected once the latest version of the ISIS CCD has been fully developed and implemented (Etoh et al. 2004). Cameras equipped with the new sensor will have an approximately four times higher resolution ($3{\cdot}10^5$ pixels instead of 80 120) and will feature an increased number of frames (144 instead of 103).

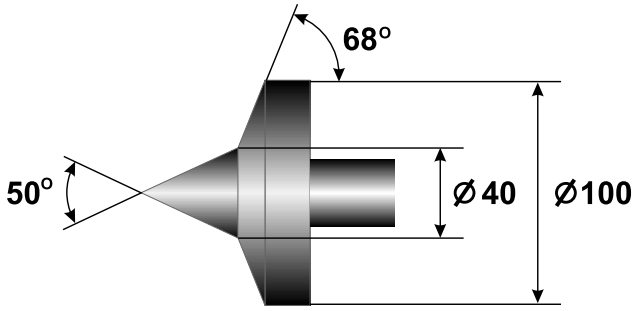

Fig. 6. Schematic of the investigated double cone geometry (adapted from Kleine and Hiraki 2004)

3 Experimental setups

The experiments were conducted in the Wind Tunnel Laboratory of the Institute of Space and Astronautical Science (ISAS) of the Japan Aerospace Exploration Agency (JAXA). The supersonic tunnel of this facility is equipped with optics for a ∅600 mm schlieren system, where the schlieren head has a focal length of 6 m. For the tests with the new high-speed color video camera, a direction-indicating color schlieren apparatus (Kleine 2001, Settles 2001) was devised and set up. In this system, the cut-off had a circular shape matching the effective geometry of the source, and astigmatism was corrected by means of a cylindrical lens in front of the source mask (Prescott and Gayhart 1951, Kleine 2001). A monochrome version of the mask, with exactly the same geometrical layout as the one for color schlieren, but with transparent instead of colored segments, was used for the tests with the Shimadzu camera. In all experiments, a flashlamp positioned behind the source mask provided intense illumination for about 1 ms. Different imaging lenses, with focal lengths ranging from 250 mm to 2500 mm, allowed one to observe either the test section in its entire diameter of 600 mm or selected portions of it. The highest magnification obtained in these trials yielded a field of view of 57 mm × 48 mm.

The primary goal of these tests was to visualize the instabilities that occur in the supersonic flow around double cone geometries. In earlier tests (Kleine and Hiraki 2004) it had been found that for the chosen double cone geometry (see Fig. 6) a pulsating instability develops for flow Mach numbers exceeding $M = 2.1$. This previous study had revealed some major features of the instability, but due to the considerably limited spatial resolution of the time-resolved records (see Fig. 3), it had not been possible to identify details of this process. The significantly higher resolution offered by the new high-speed video cameras, and the additional benefit of being able to apply color schlieren techniques, were expected to provide more detailed and informative visualization results. As the instability was known to be periodic with a frequency close to 1 kHz, a manually provided synchronized trigger signal for camera and flashlamp during the tunnel run was sufficient to capture at least one oscillation, if the recording speed was kept below or equal to 62 500 fps.

In addition to the investigation of the flow around the double cone, two other sets of experiments were conducted in order to further demonstrate the capability of the cameras when used in conjunction with a high-sensitivity/high-resolution schlieren system. It was the objective of these tests to observe in time-resolved fashion the flow fields associated with the explosion of a small firecracker and the bursting of a toy balloon. In both cases, a microphone placed in close proximity to the firecracker and the balloon, resp., provided the trigger signal for flashlamp and camera. The optical system for all tests remained unchanged, only the imaging lenses and thus the visualized field of view were modified as the flow fields of interest differed in size.

The firecracker was suspended on a thread and the fuse was lit with a lighter, while the balloon was filled with helium until it eventually burst. The inherent non-reproducibility of the explosion and the bursting process required several repetitions – approximately fifteen tests were run in each configuration.

4 Results and Discussion

Representative image sequences of the described experiments are shown in Figs. 7 to 9. The detailed description of the physical mechanisms of the observed processes, in particular the instability of the flow over the double cone,

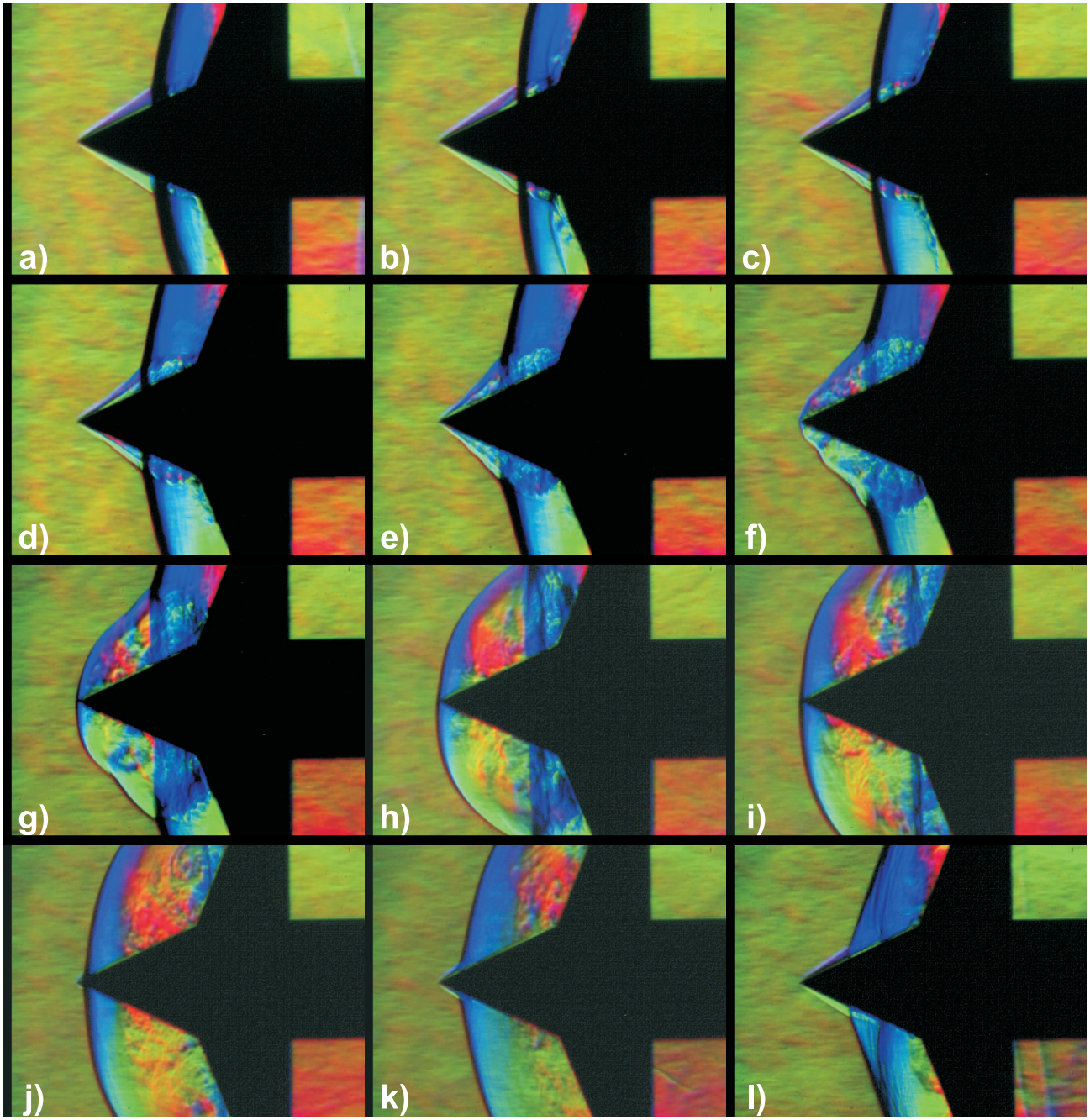

Fig. 7. Pulsating flow around the double cone model of Fig. 6, free stream Mach number $M = 3$. Time-resolved color schlieren visualization showing every seventh frame from a recording with 62 500 fps (time interval between shown adjacent frames: $\Delta t = 96\,\mu$s)

is the subject of a different paper, and only the main observations will be discussed here.

If the flow over the double cone were stable, one would expect a flow pattern similar to the one shown in Fig. 7a. The first cone (opening angle 50 °) induces a leading conical shock whose characteristics can be determined analytically (Taylor and Maccoll 1933). For the given free stream Mach number $M = 3.0$, theory predicts a shock angle of 34.5 °, which corresponds well to the observed angle in Fig. 7a. The opening angle of the second cone (136 °) is larger than the limiting angle for an attached conical shock, hence a detached bow shock with a stand-off distance determined by the free-stream Mach number is generated.

The shock wave pattern around the investigated double cone therefore consists of a leading conical shock followed by a stronger largely normal shock, as seen in Fig.7a. In previous investigations (Kleine and Hiraki 2004) it had

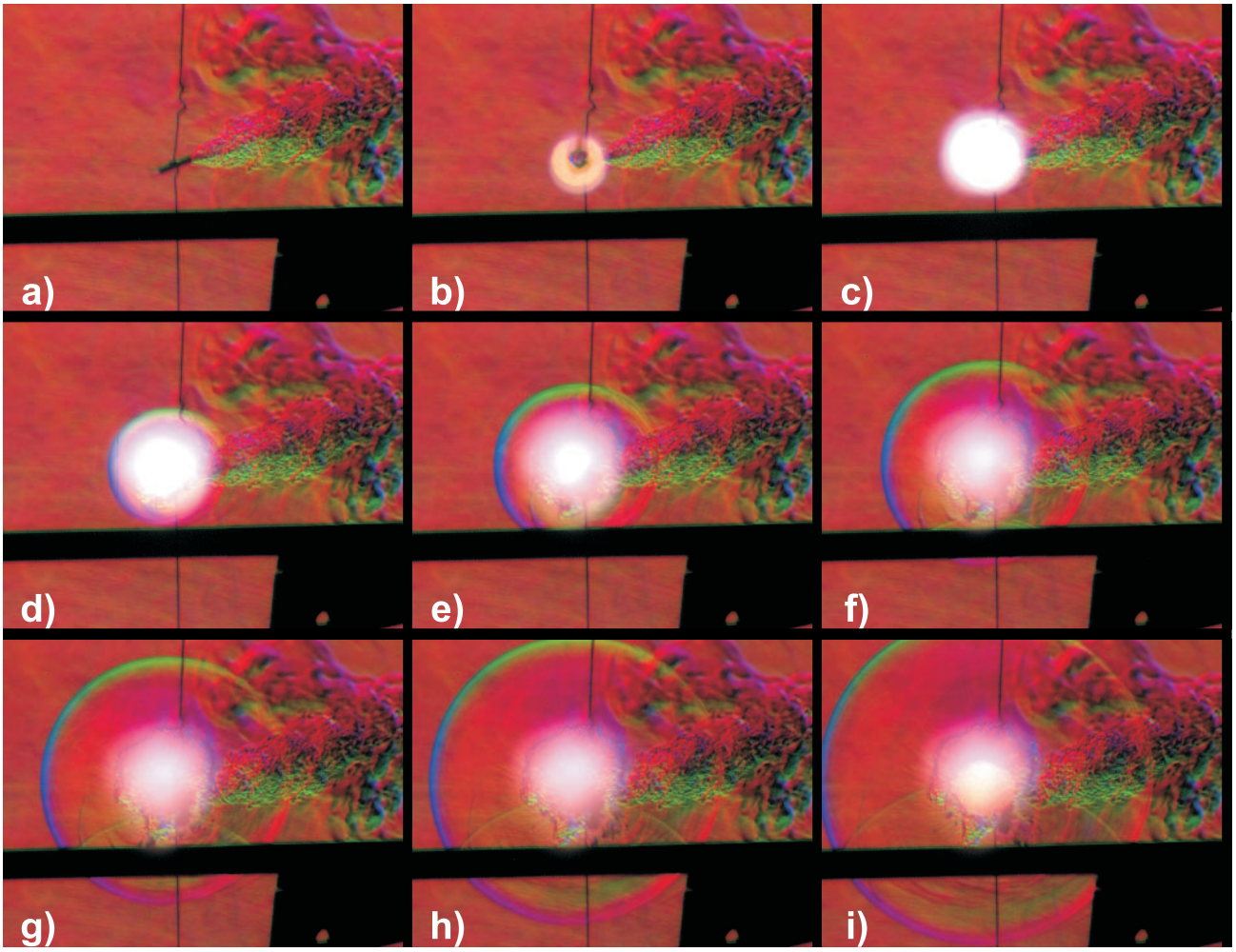

Fig. 8. Explosion of a firecracker. Time-resolved color schlieren visualization showing every third frame from a recording with 62 500 fps (time interval between shown adjacent frames: $\Delta t = 32\,\mu$s)

been shown that this shock system was stable up to Mach numbers of 2.1, but started to oscillate at $M = 2.2$. This oscillation was initially mild and involved only a relatively small movement of the shocks, but became increasingly pronounced and violent with increasing free stream Mach number. The time-resolved color schlieren visualization of Fig. 7 allows one to discern the different phases of the process in unprecedented clarity. The direction-indicating technique is particularly suited to detect vortex structures, which are represented as circular rainbow patterns (see, e.g., Fig. 7c, where two pronounced vortices are formed above the surface of the first cone between the normal shock and the face of the second cone).

Each pulsation is initiated by a disgorging of fluid from the region behind the almost normal second shock. This leads to a thickening of the boundary layer on the first cone, which in turn causes an oblique shock that moves towards the cone tip (Figs. 7b-d). The interaction of this newly formed oblique shock with the normal shock generates a growing pocket of turbulent high-pressure fluid in the region behind the normal shock, which pushes this shock slowly upstream. The normal shock appears to be continuously weakened close to the surface of the first cone, and the turbulent high-pressure fluid moves further towards the cone tip. Eventually the newly formed oblique shock reaches the vertex of the cone (Fig. 7e), where it merges with the leading shock to become temporarily one single, curved shock front (Fig. 7f). The turbulent high-pressure fluid accumulates in the transition zone between the two cones and pushes the shock front further upstream (Figs. 7g-i), until the double cone temporarily appears as a blunt body with a minute spike at the center (Fig. 7j). This pattern is, however, not sustainable as the 'cushion' of compressed fluid between the second shock and the surface of the second cone can expand in downstream direction. The complete sequence of images shows clearly how this fluid is swept up the face of the second cone and pushed over the edge into the wake (Fig. 7k). The associated drop of pressure in the shock-compressed gas allows the shock system to move again with the free-stream flow and towards the second cone in order to establish a new equilibrium position (Fig. 7l), and eventually the

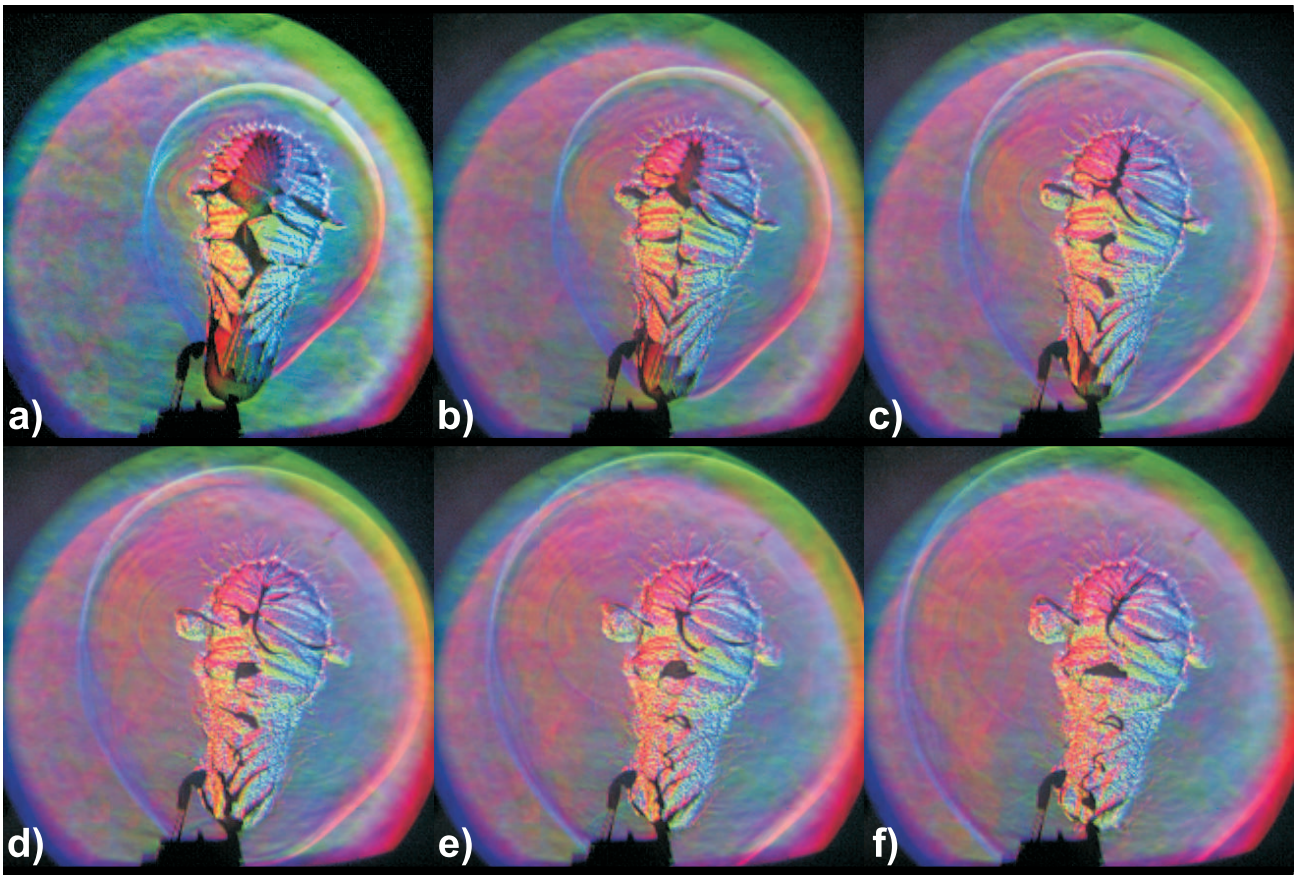

Fig. 9. Bursting of a Helium-filled toy balloon. Time-resolved color schlieren visualization showing every eighth frame from a recording with 125 000 fps (time interval between shown adjacent frames: $\Delta t = 48\,\mu$s)

shock pattern prior to the onset of the pulsation is formed again. During this process, the conical shock around the vertex of the first cone is re-established, after it had almost entirely disappeared during the forward motion of the shock system (Figs. 7f-i). The process then repeats itself in essentially identical fashion. The period of one cycle amounts to approximately 1100 μs, which corresponds to previous results (Kleine and Hiraki 2004) as well as to the characteristic time found in simultaneously conducted force measurements.

The other trials conducted in this test campaign are more of an illustrative than a scientific character, but they reveal clearly the high diagnostic potential of time-resolved color schlieren visualization. In Fig. 8, the explosion of a small firecracker (about 20 mm in length, 3 mm in diameter) is depicted. The firecracker is suspended on a thread and is positioned about 25 mm above a cylindrical microphone (seen as a black horizontal bar on each frame of Fig. 8). After the fuse has been lit, the firecracker is ignited and the ensuing fireball of combustion products drives a largely spherical shock wave. The combustion is accompanied by an intense and rather long lasting light emission. This luminous zone veils the exact formation and movement of the cloud of combustion products during the initial phase of the explosion. Only about 1 ms after ignition does the luminous zone in the center disappear. At this stage the expansion of the combustion product cloud has already significantly slowed down. The blast wave is seen to reflect from the microphone (Fig. 8f-i) before it eventually leaves the field of view. In the initial frames of this sequence, one can also discern weak waves emanating from the lit fuse prior to the ignition of the charge. One of these waves, in fact, triggered the recording of the process so that the instant of explosion could be captured.

In contrast to this, the recording of the sequence visualizing the bursting of a helium-filled balloon only started when the shock wave released by the burst reached a small microphone, seen in each frame of Fig. 9 at the lower left side of the balloon. As the bursting process was not initiated externally, i.e., the balloon was simply inflated until it burst, no other trigger signal but the ensuing blast wave itself could be provided and hence no images exist of the initial break-up of the balloon shell. The recorded sequence clearly shows how the blast wave, initially of similar outline as the pear-shaped balloon, quickly approaches a spherical contour. The plastic shell is seen to shrink rapidly, with a speed that is of the same order of magnitude as the propagation speed of the blast. The gas that filled the balloon, however, expands only slowly. Long after the shell has disintegrated and disappeared, the helium

cloud has still largely the shape of the balloon, with only local protrusions and striations that are generated by a direct interaction of the cloud with the shell fragments. As the bursting is only initiated by overpressure, small irregularities in the shell thickness become the primary influencing factors for the way in which the shell fails and subsequently disintegrates. Approximately one in ten balloons bursts in the fashion shown in this sequence, generating spine-like remnants of the shell.

5 Conclusion

The examples given in the previous section have clearly demonstrated the significant diagnostic potential that time-resolved color schlieren visualization with the help of the newly developed high-speed color video camera has. The obtained images have depicted the investigated flow fields in unprecedented clarity, and the use of color has helped to clarify the nature of some of the observed phenomena. While the system requirements, in particular with respect to an adequate light source, have been increased for this application, the results clearly indicate that this increased effort was fully justified. The tests reported here are the first successful time-resolved direction-indicating color schlieren visualizations of compressible flows with frame rates up to 125 kHz. The nature of these tests did not warrant higher frame rates, but visualizations with 1 Mfps can easily be achieved.

Acknowledgement. The authors gratefully acknowledge the assistance of K. Sato and T. Irikado in the preparation and running of the wind tunnel experiments.

References

Abe A, Ojima H, Ogawa T, Babinsky H, Takayama K (1999) Animated Display of Sequential Holographic Interferograms of Shock Wave/Vortex Propagation. In: Ball GJ, Hillier R, Roberts GT (eds.) Proc. 22nd Int. Symp. Shock Waves, Imperial College Press, pp. 1111-1116

Balch K (1997) High-speed videography. In: Ray SF (ed.) *High-Speed Photography and Photonics*. Focal Press, Butterworth-Heinemann, pp. 99-123. Reprinted by SPIE under the same title as SPIE PM120 in October 2002.

Dewey JM, Kleine H (2004) High-speed photography of microscale blast wave phenomena. In: Paisley DL, Kleinfelder S, Snyder DR, Thompson BJ (eds.) Proc. 26th Int. Congr. High Speed Photography & Photonics, SPIE, Bellingham, Vol. 5580, pp. 106-114

Etoh TG (1992) High Speed Video Camera of 4500 pps. J. Inst. Television Engineers, 46(5): 543-545 (in Japanese)

Etoh TG, Takehara K, Okinaka T, Takano Y, Ruckelshausen A, Poggemann D (2000) Development of High-Speed Video Cameras. In: Takayama K, Saito T, Kleine H, Timofeev E (eds.) Proc. 24th Int. Congr. High Speed Photography & Photonics, SPIE, Bellingham, Vol. 4183, pp. 36-47

Etoh TG, Poggemann D, Ruckelshausen A, Theuwissen A, Kreider G, Folkerts H-O, Mutoh H, Kondo Y, Maruno H, Takubo K, Soya H, Takehara K, Okinaka T, Takano Y, Reisinger T, Lohmann C (2002) A CCD Image Sensor of 1 Mframes/s for Continuous Image Capturing of 103 Frames. In: Proc Int Solid-State Circuits Conf, IEEE 0-7803-7335-9/02, pp. 45-48

Etoh TG, Hatsuki Y, Okinaka T, Ohtake H, Maruyama H, Hayashida T, Yamada M, Kitamura K, Arai T, Tanioka K, Poggemann D, Ruckelshausen A, van Kuijk H, Bosiers JT, Theuwissen AJ (2004) An image sensor of 1,000,000 fps, 300,000 pixels, and 144 consecutive frames. In: Paisley DL, Kleinfelder S, Snyder DR, Thompson BJ (eds.) Proc. 26th Int. Congr. High Speed Photography & Photonics, SPIE, Bellingham, Vol. 5580, pp. 796-804

Fuller PWW (1997) The development of high-speed photography. In: Ray SF (ed.): *High-Speed Photography and Photonics*. Focal Press, Butterworth-Heinemann, pp. 7-28. Reprinted by SPIE under the same title as SPIE PM120 in October 2002.

Honour J (2000) A High Resolution Electronic Imaging System for Schlieren Recording. In: Takayama K, Saito T, Kleine H, Timofeev E (eds.) Proc. 24th Int. Congr. High Speed Photography & Photonics, SPIE, Bellingham, Vol. 4183, pp. 163-169

Kleine H (2001) Flow Visualization. In: Ben-Dor G, Igra O, Elperin T (eds.) *Handbook of Shock Waves*, 1, 683-740, Academic Press

Kleine H, Takayama, K (2001) Recent Improvements and Enhancements of Density-Sensitive Flow Visualization Methods. In: Proc. 1st Int. Symp. Advanced Fluid Information, Tohoku University, pp. 551-558

Kleine H, Takayama K (2002) Current Status of Time-Resolved Visualisation of High-Speed Compressible Flow. In: McIntyre T (ed.): Proc. 3rd Australian Conf. on Laser Diagnostics in Fluid Mechanics and Combustion, University of Queensland, p. 121

Kleine H, Hiraki K (2004) Supersonic flows over double cone geometries. In: Jiang Z (ed.) Proc. 24th Int Symp Shock Waves, paper 2951 (CD proceedings)

Maruyama H, Ohtake H, Hayashida T, Yamada M, Kitamura K, Arai T, Tanioka K, Etoh TG, Namiki J, Yoshida T, Maruno H, Kondo Y, Ozaki T, Kanayama S (2004) Color video camera capable of 1,000,000 fps with triple ultrahigh-speed image sensors. In: Paisley DL, Kleinfelder S, Snyder DR, Thompson BJ (eds.) Proc. 26th Int. Congr. High Speed Photography & Photonics, SPIE, Bellingham, Vol. 5580, pp. 244-249

Prescott R, Gayhart EL (1951) A Method of Correction of Astigmatism in Schlieren Systems. J.Aer.Sci. 18(1), 69

Ray SF (ed.) (1997) *High-Speed Photography and Photonics*. Focal Press, Butterworth-Heinemann. Reprinted by SPIE under the same title as SPIE PM120 in October 2002.

Reichenbach H (1981) Stowellen in Luft - Ausbreitung von Stowellen in einem Tunnel mit Verzweigungen. IWF, Göttingen, E 2581.

Settles GS (2001) *Schlieren and Shadowgraph Techniques*. Springer Verlag, Heidelberg, New York

Taylor GI, Maccoll JW (1933) The Air Pressure on a Cone Moving at High Speed. Proc. Roy. Soc. (London) A, 139(838):278-311